CHAPTER 7

7 Uptake of Arsenic by *Navicula sp.* into cellular components: An X-ray energy dispersive study

7.1 Introduction

The living world offers many examples of organisms that present order and regularity of shape, with patterns that are often like lattice patterns of minerals. Both fresh water and marine ecosystem have plenty of these organisms that synthesize an external inorganic causing (from micro- to macrostructures) and an intercellular nanostructure. Among them, the diatoms have most important impressive architecture because of their highly elaborate exoskeleton. The highly structured silica nanopore in the skeleton of the diatoms is the target of many researchers.

Diatoms are microscopic (~1–500 μm in length) single-celled algae with characteristic rigid cell walls (frustules) composed of amorphous silica. They are ubiquitous organisms found in a wide variety of habitats and are thought to be responsible for up to 25% of the world's net primary production of organic carbon [1]. There are currently estimated to be over 100, 000 different species, classified by their unique frustule morphologies [2]. Diatoms are one of the major groups of microalgae, which are divided into two categories: centric diatoms and pennate diatoms.

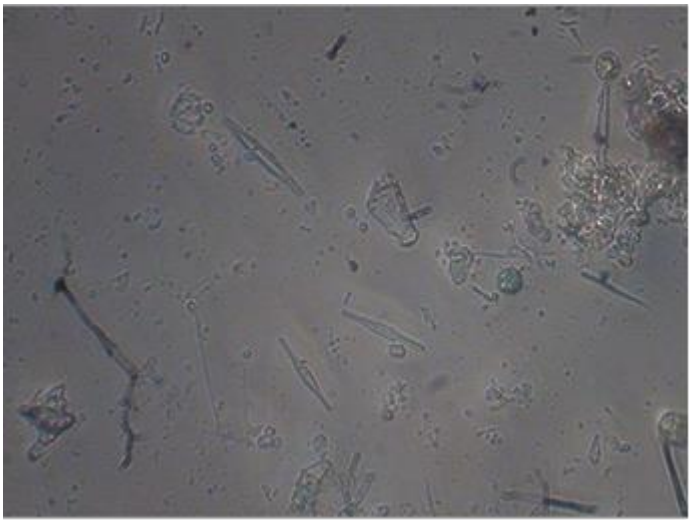

Figure 7.1 Diatoms in the environment (Source: Author)

Diatoms are usually classified as one of two main groups depending upon the symmetry of their frustules. Depending on the shape and symmetry, two types

of diatoms are recognized: the pennate and centric forms. Pennate diatoms have elongated or "boat-shaped" valves with a bilateral symmetry. They are mostly benthic, but few planktonic genera may be abundant in the plankton. Centric diatoms have a radial symmetry and are much more common in the plankton. Along the length of its frustule, pennate diatoms have a long slit known as the raphe, which helps in their motility and attachment to substrata. Pennate diatoms tend to be elongated and generally have parallel striae (furrows or rows of holes in the silica) arranged normal to the long axis [3, 4]. The spacing between adjacent striae is species specific and typically varies from ~0.3 to 2 µm. The lines of silica between the striae are called costae. Costae tend to be arranged in combs or other space-filling patterns such as honeycombs, which possess remarkably uniform pores. Aside from their symmetry, frustules display an unparalleled diversity in structure and morphology, and this may be exploitable in nanotechnological applications.

Diatoms are usually classified as one of two main groups depending upon the symmetry of their frustules (**Figure 7.2**).

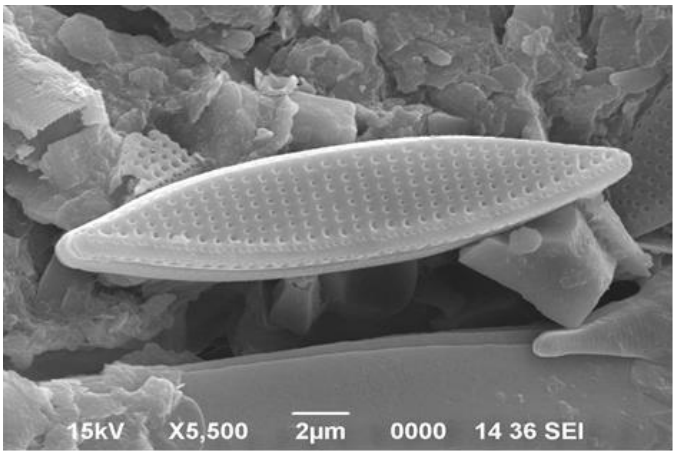

Figure 7.2 SEM image of a pinnate diatom of *Navicula* species (Source: author)

Diatoms are unicellular microalgae that form micro scale silica cell walls exo-skeleton (called frustules) comprised of diverse and highly ordered three dimensional porous silica structure and that hold considerably promise for biological or fabrication of nanostructured materials and devices. These patterns are species-specific and are faithfully reproduced upon cellular reproduction. The wide diversity in diatom species, each with a unique shape, size, pore size and architecture offers a huge selection for device and device applications. Diatoms (Bacillariophyceae) are microscopic unicellular algae abundant in almost all

aquatic habitats; they are key components of food webs in mostly all fresh water and saline environment [5].

Diatoms have varied life strategies including floating in the water column (phytoplankton), colonizing submerged surfaces and living within the surface of deposited sediments. Some cells are essentially cylindrical (centric) while others have an elongated "boat-like" shape. Since they are algae belonging to the division Bacillariophyta they require light for photosynthesis. Perhaps the most studied group of diatoms belongs to the phytoplankton. Phytoplankton diatoms rely on fresh water/ocean currents and wind to keep them in the upper water levels as their cell wall is denser than water around them.

7.1.1 Frustule formation

The process of frustule formation is not well understood but is thought to involve the diffusion-limited precipitation of silica [6]. Amorphous silica particles of relatively low molecular weight and ~1–10 nm in diameter are thought to be transported to the periphery of the silica deposition vesicle (SDV) by silica-transport vesicles (STVs). Once released inside the SDV, the particles diffuse until they encounter part of the growing aggregate, to which they adhere. The surface of the particles is thought to consist mainly of silanol groups [$Si(OH)_2$ or Si–OH], which enable them to diffuse over the surface of the aggregate in a process termed sintering [7]. This surface migration allows the molecules to reorganize their positions towards thermodynamic equilibrium, usually resulting in a smoothing of the aggregate surface. Sintering has been shown to be affected by factors such as pH and temperature, which may explain the changes in frustules morphology observed when a single diatom species is grown under varying conditions [8, 9]. After deposition and a period of surface relocalization, the silica morphology becomes stabilized in a process that may involve an inorganic cation such as aluminium. Although little is known about how the silica is transported to the SDV, microtubules have been found to be associated with the developing SDV [10]. Recent computer simulations imply a role for these microtubules as carriers for the STVs; the arrangement of the microtubules may thus account for the gross morphological characteristics of the frustule (i.e. the micrometre level of order), each costa being associated with the site of release of STVs being transported by an individual microtubule.

Valve formation begins within the mother cell where each of the two new daughter cells develop a new hypovalve and girdle bands in a special cellular compartment, the silicon deposition vesicle (SDV). During the growth and maturation of the new valves, silicon transport vesicles (STV) are used to transport silica precursors to the SDV from the cytoplasm. The STV's fuse continuously with the expanding SDV, until the valves, hymen and girdle bands, are excreted. Before excretion the siliceous parts are coated with a protective layer of proteins and carbohydrates that stop spontaneous dissolution of the valves in the aqueous environment [2, 11].

7.1.2 Arsenic sorption by algae

Arsenic (As) is a widely distributed metalloid in natural ecosystems, and it is considered a priority pollutant [12]. Arsenic and its compounds have been widely used in pigments, as insecticides and herbicides, as an alloy in metals and arsenic compounds were developed as chemical warfare agents. The toxicity of arsenic increases greatly when arsenic is reduced from a +5 to a +3 oxidation state. Ferguson et al. [13] discuss the interesting chemistry of arsenic with oxidation-reduction, ligand exchange, precipitation and adsorption reactions all taking place. Arsenic forms kinetically stable bonds with sulfur and carbon in organic compounds. Like mercury, arsenic (+3) reacts with sulfhydryl groups of cysteine in proteins. Arsenate, the stable form in aerobic water, may be removed by several mechanisms. *Codium taylori* (a green alga), showed higher arsenic (+3) uptake (90 mg g^{-1}) at acidic p^H (2-4) values.

Algae are known to be able to accumulate heavy metals. They are able to eliminate metal ions from aquatic solutions in a short time by biosorption in a complicated system, without any toxicity problem. It is an important biochemical function of algae in the shaping of proper ecological relationships and interaction between organisms in the aquatic environment.

The use of aquatic algae is often advocated for bioremediation of arsenic contaminated waters as they absorb arsenate and transform it into arsenite and methylated chemical species. Algae mistake As^V for $PO_4^{3-}$and actively absorb it via the same pathways. Once inside the algal cells, AsV becomes toxic as this resemblance breaks down, and algae reduce AsV to As III, methylate it to MMAA III and DMAA III, and excrete it mostly as AsIII and/or DMAAIII, which is thought to be a detoxifying mechanism [14, 15, 16]. Arsenate and arsenite were

the dominant species in the freshwater algae *Synechocystis* and *C. reinhardtii* [17, 18]. This transformation reaction is suggested to be correlated with algal growth rate and P nutrient status, leading to almost complete methylation under P-limiting conditions and slower methylation and excretion of AsIII into the media if P is in excess [14]. Nonetheless, these studies confirm that P has a key role in arsenate toxicity and that biotransformation of As by algae is a central component of aquatic As cycling. Indeed, the use of algae is often advocated for bioremediation of As contaminated water [15, 16, 19, 20, 21]. Arsenate As(V), the main form of arsenic in aerobic environments and is taken up into cells by phosphate transporters [22]. Toxicity of arsenic is reduced due to its conversion from inorganic to organic form and is increased by its reduction from arsenate to arsenite for most biological system. Most diatoms, dinoflagellates and macroalgae as well as freshwater higher plants release such protein-bound arsenic as a result of sequential methylation and adenosylation. Ultimately the products are trialkylarsine oxides, innocuous substances which are slowly or not-at-all metabolized by herbivorous animals or bacteria.

In case of diatoms, changes in morphology and increase in cell size are the main manifestation of high concentration of metals [23]. Literature data on the toxicity of arsenic to freshwater microalgae are limited to chlorophytes and cyanophytes. Reported IC50 values (concentration to cause a 50% inhibition of growth) range over five orders of magnitude, from 0.048 to 202 mg/L [24, 25, 26] and are generally well above environmental concentrations of arsenic. The wide variability in sensitivity to arsenic is likely due to biotic factors such as species type, differing uptake/exclusion pathways, detoxification mechanisms and prior-exposure, as well as abiotic factors such as arsenic species, phosphate concentrations, pH and exposure time.

Field studies dealing with metal contaminations in various regions and countries have shown quite consistent responses of diatom communities [27] such as higher abundances of small-sized species [28, 29] increasing proportions of metal-tolerant species, or significantly higher occurrences of valve deformities. Metal toxicity in diatoms is linked to different steps in the circulation of the toxicant both across the membrane (especially with respect to the uptake mechanisms) and inside the cell (e.g., nuclear alterations), thus inducing

perturbations in the normal functioning of structural and functional intracellular components.

X-ray microanalysis is a good complement to other methods in pollution studies.

According to Pedersen et al. [30], the advantages of the X-ray microanalysis method are –

1. All elements are analyzed simultaneously, which allows the easy detection of 'unexpected' pollutants,
2. Only a small amount of material is needed for analysis, so that also algae of which only small quantities can be collected, can be analyzed,
3. Examination in the electron microscope allows discrimination between different species and between cells and non-living particulate matter in inhomogeneous samples**.**

X-rays emitted on the interaction of the electron beam with the specimen have energies that are characteristic of the elements from which the X-rays are generated. The collection of the X-rays enables the investigator to determine the elemental composition and distributions of the specimen being examined in the scanning electron microscope (SEM) [31]. In addition to rapid qualitative analysis, accurate quantitative analysis can also be achieved with Energy Dispersive X-Ray Spectrometer (EDS) [32].

The capacity of diatoms to accumulate metals from water producing an internal concentration greater than in their surroundings has been reported and discussed in literature [33, 34]. The ratio of CFs (Concentration Factors) quantifies this ability to concentrate metals in plankton and epilithic diatoms have been proved to show high CFs [35]. Uptake of pollutants from surrounding water by algal cells could be the results of many processes. The chemical compound may be metabolically active, which can act as an essential nutrient or mineral and be transported across the cell membrane and thus enter into biochemical process [36]. In case of metal, Cambell et al. [37] recognized the interaction of metal with an algal cell with thus normally involve the following steps: i) diffusion of the metal from the bulk solution to the biological surface; ii) sorption/ surface complexation of metal at passive binding sites within protection layer, or at sites on the outer of surface of the plasma membrane; iii) uptake or “internalization” of the metal (transport across plasma membrane).

In contrast to organic contaminants, heavy metals/metalloids persist and are likely to accumulate in the environment. Recently, heavy metal/metalloid biosorption using biological material has emerged as a potential alternative instead of the existing conventional physicochemical methods [38, 39, 40]. Among the biological material, algae have proved to be advantageous because they present several advantages, i.e. economic regeneration, metal recovery potentiality, lower volume of chemical and / or biological sludge to be disposed of, high efficiency in dilute effluents and large surface area to volume ratio [41].

7.1.3 Arsenic accumulation by Diatoms

Dissolved arsenic in the solution are also taken up by diatoms because arsenate is similar to phosphate in size, geometry and its ability to enter into biochemical reactions. Studies of the accumulation of arsenic in diatoms and macroalgae experiments showed that arsenic uptake is related to the prevailing phosphate concentration. Phosphate present at low levels often does not influence arsenate uptake. Arsenic uptake increases as phosphate uptake increases until a threshold value is reached and arsenic uptake is inhibited. The increased uptake of arsenic as phosphate uptake increases at low phosphate concentrations is attributed to increasing phosphate metabolism and indiscriminate arsenate uptake. Arsenate may enter cells by transport mechanisms unable to discriminate between phosphate and arsenate. Under phosphate stress arsenic is concentrated, converted into non-toxic products and excreted [42].

Various authors used microscopic techniques (TEM, SEM, Environmental SEM, and Environmental TEM) to localized metals within the biofilm matrix or in diatoms [43, 44, 45, 46]. Lai et al. [47], Chien [48] and Nakanishi et al. [49] showed that heavy metal elements could be found in diatom species such as *Nitzschia palea*, *Fragilaria tenera*. etc. by using X-ray analysis to observe metals contained in algae collected from heavy metal pollution sites. Research on the use of diatom *Navicula* sp. for remediation environmental pollution were also had been conducted for Cd only. But, research on the use of local diatom to reduce the concentration of Arsenic (As) had not yet well developed. Therefore, this research was conducted in order to find out the effect of 3mg/L, 8 mg/L, 14 mg/L and 55 mg/L concentrations of As on the diatom *Navicula* sp. population growth and its accumulation. A laboratory experiment was developed with those different concentrations with 3 replications and control. ANOVA was performed for all the

data to confirm their validity using SPSS 18.0. A probability of 0.05 or lower was considered as significant (Data were given in Annexure III).

In this study the response of diatom growth rate and valve malformation to contamination with the arsenic was tested. This study aims to ensure the question of whether diatoms can accumulate As from the solution. In this investigation X-ray microanalysis was applied to studies of metal accumulation in freshwater diatom *Navicula sp.* in a hydroponic As environment.

This study will be important for the exchange of epiphytic diatom composition in heavy metal contaminated aquatic systems, to determine heavy metal tolerant species. In this study the response of diatom growth rate and valve malformation to contamination with the arsenic was tested. Study of the effects of metals on biological activity in the aquatic environment can potentially be used as a basis to find metal contaminated sites with the help of a diatom indicator. Our goal was to understand the physiological responses of diatom *Navicula* sp. an important and abundant species of freshwater diatom to arsenic contamination.

In detail, this study tried to find the answer on the following two hypothesizes:

1. The culture of benthic diatoms is possible under the given laboratory (artificial) conditions.
2. High concentrations of As (55 mg/L As) decrease the number of benthic diatoms and increase abnormalities in cell walls.

7.1.4 Metal-cell interactions

Diatoms are known to have a high affinity towards a variety of dissolved elements and they will therefore exert a strong control on the transfer of heavy metals along the water column to the sediments. Algal cell walls are surrounded by a three-dimensional network of macromolecules (polysaccharides and proteins). These carry negatively charged functional groups such as carboxyl, hydroxyl, phosphate or amine groups. Since metal ions in water solution generally are in cationic form, they are adsorbed to the algal cell walls. The algal metal biosorption is pH dependent and in general, acidic conditions of pH 3–5 are most favourable for the sorption of metal ions [50, 51].

The toxicity and uptake of metals by phytoplankton cells are processes that are highly dependent on the specific interaction chemistry between the metals in

question and the elemental composition and thickness of the cell surface. Gélabert et al. [52, 53] demonstrated that the main contribution of metal adsorption came from the organic layer covering the frustules as compared to the frustule itself. This layer contains a variety of functional groups including carboxyl ($-COO^-$) and silanol ($-SiO^-$) groups that can bind metal ions and, which under normal freshwater pH-values, provide the cellular surface with an overall negative charge [52, 53]. Various studies on cell surface-metal interactions suggest that carboxyl groups contribute to the major part of proton and metal binding sites [52, 54].

7. 2 Materials and methods

7.2.1. Cell collection and culture

The living fresh water diatoms are collected from the catchment ponds of a water purification plant in Assam, India during September – November, 2010. Epiiphitic diatoms were collected from macroalgae, while epilithic diatoms from different stones in the pond. The collected pinnate diatom species were cultured in the Tissue Culture Laboratory (Department of Molecular Biology and Biotechnology, Tezpur University, Assam, India) under controlled conditions [temperature 25±0.50C/20±0.50C day/night cycles; photoperiods 16 hr light (fluorescent lamps) and 8 hr dark period] in the WC medium proposed by Guillard and Lorenzen [55]. The protocol was slightly modified by doubling the composition of sodium meta silicate and lowering the P^H from 7 to 6.23 hence making the culture media acidic [56]. The freshwater diatoms are cultured both in the solid and liquid media.

Table 7.1 Major nutrients and micronutrients for freshwater "WC" medium

Compositions	**Amount**
Major nutrients(in mM)	**(mg/L)**
$CaCl_2.2H_2O$	36.76
$MgSO_4.7H_2O$	39.97
$NaHCO_3$	12.60
$Na_2SiO_3.9H2O$	56.84
K_2HPO_4	8.71
$NaNO_3$	85.01
Micronutrients (in µM)	
Na_2EDTA	4.36
$FeCl_3.6H_2O$	3.15
$CuSO_4.5H_2O$	0.01
$ZnSO_4.7H_2O$	0.022
$CoCl_2.6H_2O$	0.01
$MnCl_2.4H_2O$	0.18
$Na_2MoO_4.2H_2O$	0.006
H_3BO_3	1

These are dissolved in 100 ml of sterile water. Major nutrients are prepared in 1L distilled water then 1ml of it was removed and 1ml of micronutrients is added to it.

[b] Then the pH of the media was lowered from 7 to 6.23 by adding HCL/NaOH and [c] the media was autoclaved at 120^0c for 20 minutes.

[d] After autoclave, vitamins as shown below:

Vitamins:

ThiaminHCL= 0.1mg/L [T100 micropipette]

Biotin = 0.5µ g/L [T20micropipette]

B_{12} = 0.5 µ g/L [=29ml water+ 1ml B_{12} -5 ml) were added in the same proportions to the media (**Table7.1**).

[e] Then the media was inoculated with the environmental samples containing the micro-algae.

7.2.2. Frustule Isolation

In order to analyze the diatom frustules by scanning electron microscopy (SEM) and to remove the external organic matrix covering the frustules, a cleaning procedure was needed that removed the external organic matrix covering the frustules.

In our work, this was done by using the following procedure

(a) Culture flask was shaken for 5 minutes to detach all diatoms;

(b) 10 ml of sample was centrifuged at 5000 rpm for another 10 min;

(c) The pellet was washed in double distilled water three times to remove the excess of fixative;

(d) 37% aqueous HCl was added and centrifuged at 3000 rpm for 10 minutes and was put in water bath for 15 min at 60^0C;

(e) The acid was pipetted and pellet was washed again in double distilled water 3 times. Cleaned frustule valves were then stored in ethanol to avoid contamination and bacteria growth.

Diatoms were scraped from dish by using a blade, washed and then diluted in 100 ml of mineral water. Obtained diatom samples were then divided into three fractions for various analyses. The first fraction (5ml) was preserved with formalin solution (Formaldehyde 37%) for diatom identification. The second fraction (20ml) was filtered through a GF/C filter using an aspiration pump for chlorophyll

a measurement. The remaining of the samples (20ml) was used to determine the total amount of metal accumulated in diatom according to the methods followed by [57] and [58]. Each filtered with an aspiration pump through a tared metal free paper (0.45 µm membrane, Millipore) to obtained the dry weight after 60^0 C for 48 hours in incubation tube. Scanning Electron microscopy: X-ray microanalysis was carried out with two types of specimens- 1. Air-dried samples for analysis of whole cells, 2. Thin sections of fixed and embedded material to localize the metals within the cells. This high accelerating voltage was chosen to excite the K-lines of As.

7.2.3 Metal accumulation

We cultured the freshwater diatom and added the As solution to the growth media at varying concentrations. The diatoms were digested first in HNO_3 to isolate the organic material and then in NaOH to dissolve the silica frustules. Each fraction was subsequently analysed by ICP-OES for As accumulation. Our results will aid in quantifying the amount of As that diatoms take up from their surroundings and determine whether As is stored in the body or in the diatom frustules.

After 21 days of As exposure, the algal cells were filtered on a 0.45 µm Millipore filter, the resulting filtrate was acidified with ultrapure nitric acid and stored in the refrigerator before the analysis. The determination of As in the filtrate (free metal) was performed by ICP-OES (Perkin Elmer Optima-2100) [Metal accumulated] = [total metal] (applied) - [free metal] [59].

Arsenic concentration in water samples were analyzed through three replicates, filtered (0.2 µm Millex® Millipore) and mineralized with nitric acid (HNO_3 2%) before measurement. Sample from third fractions were filtered through a tared metal free paper (0.45 µm membrane, Millipore) to obtained the dry weight after drying at 60^0 C for 48 h in incubation tube. Dried biofilm samples were first digested with nitric acid (3ml HNO_3, Merck) in a pressurized medium at 100^0C for 3 h. The digestates were diluted with 20ml ultrapure water and filtered water samples were measured by ICP-OES for As analysis.

7.2.4 Chlorophyll extraction

Samples were filtered onto a glass fiber filter (GF/C, 25m; Whatman) and then kept at -200 C until analysis. Chlorophyll extraction was performed in 10ml of 90% acetone and kept 24 hours at 40C. The absorbance of chlorophylls a, b and c were read simultaneously at 630, 647 and 665nm with a spectrophotometer.

Chlorophyll values were calculated using the equation of [60]

Chlorophyll a= 11.85 E664 – 1.54 E647 – 0.08 E630

Chlorophyll b= - 5.43 E 664 + 21.03 E 647 – 2.66 E 630

Chlorophyll c= - 1.67 E 664 – 7.60 E 647 + 24.52 E 630

Values were expressed as µg chlorophyll $(10^6$ cells$)^{-1}$

7.2.5 Bioconcentration Factor

The bioconcentration factor (BCF) was used to assess the accumulation efficiency of the heavy metals, by comparing the concentration in the biota with the concentration in the external medium [61]. A BCF greater than 1 indicates that the periphyton enriched heavy metals from the water.

$BCF = C_{org} / C_{medium}$

C_{org} was heavy metals concentration in *Navicula* sp.

C_{media} was As concentration in the culture media.

Bioconcentration Factor (BCF) was calculated to determine the As accumulation in the *Navicula* sp.

7.2.6 Characterizations

Various analytical techniques are used to determine the As binding mechanisms to the diatom *Navicula*. These are as follows

SEM-EDX

Diatoms were analysed by means of SEM, which provides three-dimensional images of diatoms, useful for taxonomic identification. Our goal was to understand the physiological responses of diatom *Navicula sp.*, an important and abundant species of freshwater ecology to arsenic contamination. Scanning electron microscopy (SEM, JEOL) was used to observe the morphology of diatoms before and after As treatment.

FTIR

Fourier transform infrared spectroscopy (FTIR) analysis of diatom particles was used to determine functional groups on their surface after As modification. A KBr pellet was prepared using a 1/100 proportion of diatom particles/KBr.

XRD

X-ray powder diffraction (XRD, Rigaku D/max-2000 diffractometer) was used to characterize the crystallographic structure of diatom samples.

Zeta Potential

Zeta Potential study was determined by Micro-meritics, Nano-plus Zeta/Nano particle analyzer.

7.3 Results

7.3.1 Diatom growth

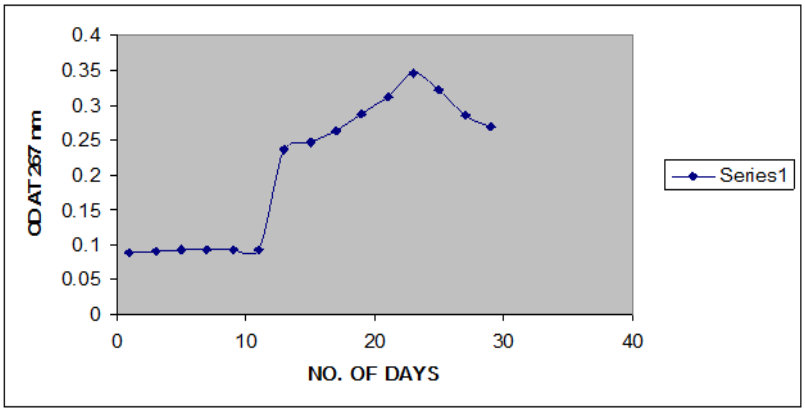

Figure 7.3 Growth curve of the *Navicula* sp.in WC media

Growth curve shows that the culture reached its maximum concentration at 23rd day. After the 23rd day, the concentration of cells decreased.

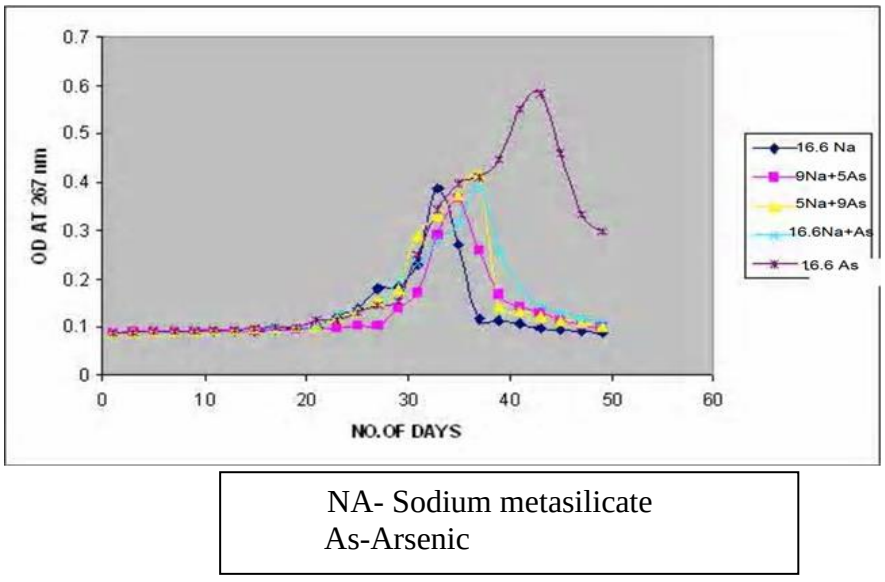

NA- Sodium metasilicate
As-Arsenic

Figure 7.4 Growth Curve of different Subcultures of diatom *Navicula* sp.

Growth curve shows that the different subcultures reached its maximum concentration at different days. The one with media containing only Arsenic took more time to reach the maximum concentration (43 days) but in addition to that, it has also shown the maximum

concentration accumulation as compared to other subcultures. From the **Figure 7.4** it was shown that at high concentration of As (55mg/L) the growth of the diatom species decline which also causes the longer time for their growth.

7.3.2 Chlorophyll extraction

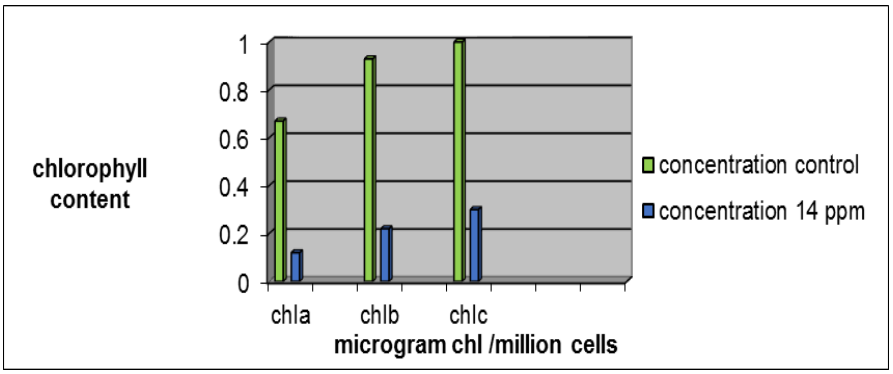

Figure 7.5 Variation of chlorophyll with As concentration

Epiphytic diatoms showed a decrease in both the total organism and the contents of chlorophyll compared to the control group.

7.3.3 Species abundance

(**A**)

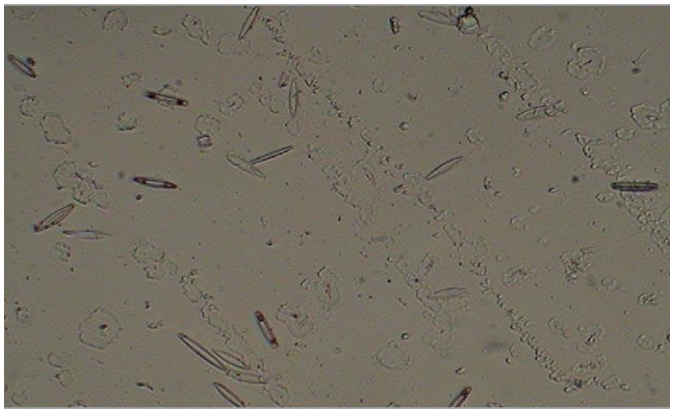

(**B**)

Figure 7.6 Living diatoms seen in light microscope. *Navicula* sp.; Microscope magnification was set on 400 times. Diatom growth in Control media (A) and As containing media (B)

The increased abundance of the *Navicula* sp. was seen in control group (**Figure 7.6A**). The effects of high As concentration (55mg/L) in the solution showed that most of the species initially present are reduced that is decline in diatom abundances, decrease in species richness, elimination of many species from the medium) (**Figure 7.6B**) and it is in agreement with the observations of Ivorra et al. [62].

Soeprobowati and Hariyati [63] had shown that the population growth of *Porphyridium cruentum* was high in the concentration of 1 mg/L Pb^{2+}, Cd^{2+}, and Cu^{2+}. In the concentration of 3 mg/L Pb^{2+}, Cd^{2+}, and Cu^{2+} had reduced the population and in the concentration of 5 mg/L had limited the population growth related to the toxicity of those heavy metals [64].

7.3.4 Bioconcentration Factor (BCF)

The bioconcentration factor (BCF) was used to assess the accumulation efficiency of the heavy metals, by comparing the concentration in the biota with the concentration in the external medium [61]. A BCF greater than 1 indicates that the periphyton enriched heavy metals from the water.

Bioaccumulation was usually used to identify worse impact of the environment to organism [65]. BCF was calculated as the ratio of the trace element concentration in the microalgae at harvest to the concentration of the element in the external environment.

Table 7.2 As accumulation by *Navicula* sp. at different period of their growth after ICP-OES analysis

As concentration (mg/L)	1st day in solution (mg/L)	5th day in solution (mg/L)	15th days in solution (mg/L)	21st days in solution (mg/L)	In *Navicula* sp.(mg/g)	BCF
3	2.1± 0.1	1.5 ± 0.1	1.2 ± 0.05	1.2 ± 0.15	0.2 ± 0.005	0.06±0.01
8	5.4± 0.2	5.3±0.05	2.15±0.01	1.22±0.005	2.09±0.01	0.26±0.01
14	12.9±0.2	11.7±0.1	11.0±0.1	5.6±0.17	4.22±0.02	0.3±0.005
55	53.3±0.15	51.3±.36	48.3±0.64	40.0±0.2	15.96±0.03	0.29±0.01

Data are mean of three replicates; ± is the standard deviation.

The accumulation of As from solution by *Navicula* sp. at different period of their growth were significant ($p<0.05$). From the above **Table 7.2**, it was seen that the BCF values of diatom *Navicula* sp. were 0.06, 0.26, 0.30 and 0.29 in 3, 8, 14 and 55 mg/L As concentrations respectively. According to Roosens et al. [65]

hyperaccumulator are plants (including microalgae, like diatoms) which have the potential to uptake and retain large quantities of metals into their cell quite suitable for phycoremediation process. A hyperaccumulator should be able to concentrate at least 1mg/g Ni, Co, Cr, Cu, Pb and 0.1 mg/g As and Cd in their cells. So, we can conclude that the diatom *Navicula* sp. is a good accumulator of As from the nutrient solution.

7.3.5 ICP-OES study

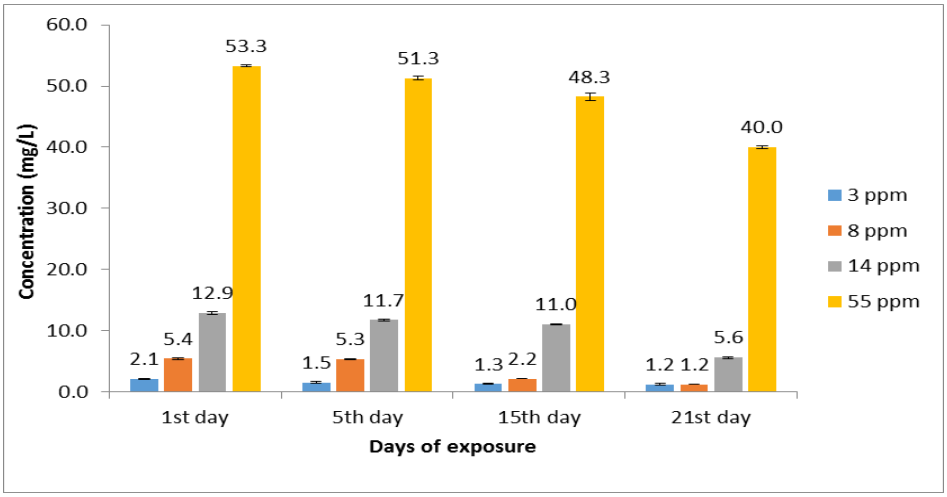

Figure 7.7 As accumulation in *Navicula* species (Statistical data in Annexure III, Table 7.3.5.1-Table 7.3.5.4)

From the ICP-OES study it was seen that there was a decreasing trend of As concentrations in all nutrient media (**Figure 7.7**).

7.3.6 SEM/EDX

The surface morphology of algae was observed using scanning electron microscope (SEM). After drying, the samples were observed using the JEOL scanning electron microscope (20 kV). To determine the chemical composition, Energy dispersive X-ray spectroscopy was performed on algae after metal adsorption. The samples were prepared as for SEM analyses. High silicon amounts were observed in the regions where the diatom outer shells were present, due to the fact that silicate groups are the principal components of these microorganisms (**Figure 7.8**).

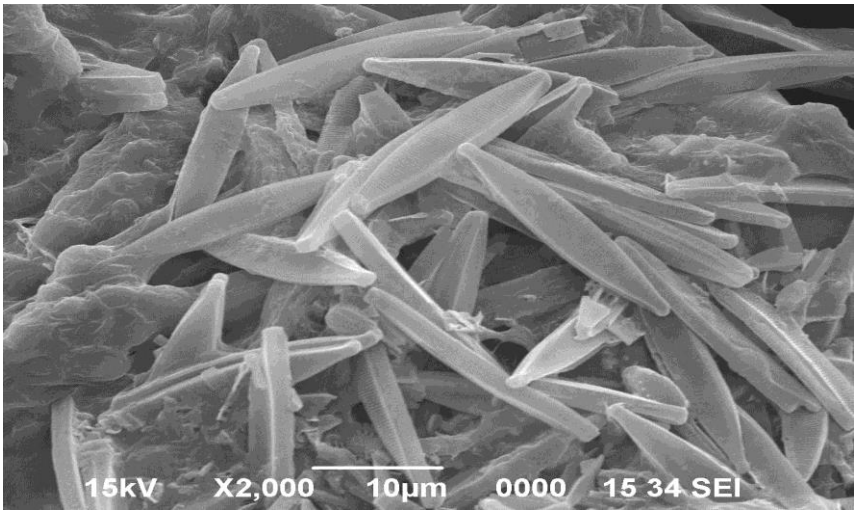

(**A**)

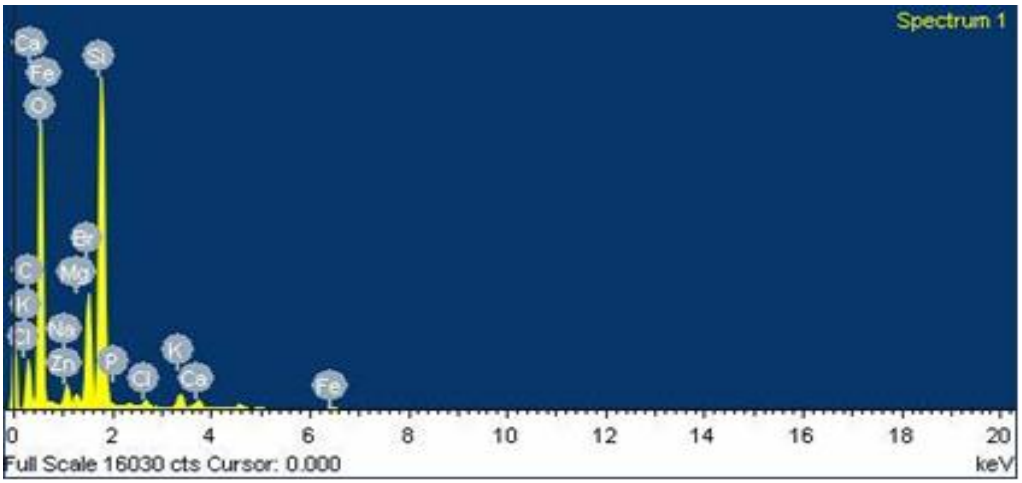

(**B**)

Figure 7.8 SEM micrograph of control group of *Navicula* colony (A); An X-ray emission spectrum from an unexposed diatom sample showed no As peaks (B)

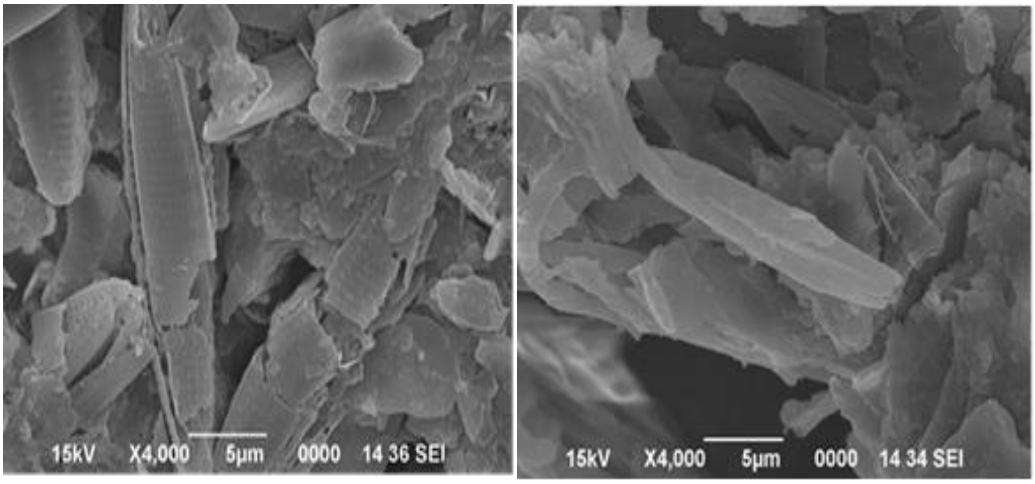

(**C**) (**D**)

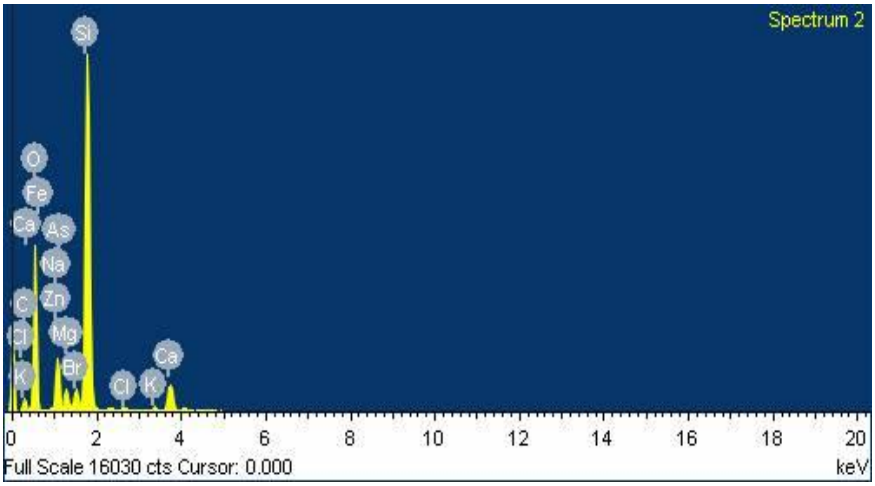

(E)

Figure 7.8 SEM micrograph of As treated of *Navicula* colony (C, D); An X-ray emission spectrum from an As exposed diatom sample showed As peaks (E)

Toxicity and accumulation of arsenic in freshwater diatom biofilm studied in the experiment showed that As exposure promoted abnormal diatom valves development, diminished biofilm biomass as well as diatom densities. It can be verified by the SEM image as shown in **Figure 7.8(C, D)**. SEM observation revealed unsuspected abnormalities in the raphe structure of many diatoms exhibiting a normal outline of the valve.

Damage to the cytoskeleton causing malformation of the raphe might compromise the nanoscale uniformity of the pore architecture: according to Mayama and Kuriyama [66] deformation of areolae or striae patterns as well as other abnormalities occur later in development; they may be secondary effects controlled by oxidative stress induced damage to cytoplasmic components involved in macromorphogenesis [67].

Perez and colleagues [68] found that total abundance of diatoms decrease linearly with respect to increasing copper concentration. Moreover, community structure may be affected by metals; Sanders and Cibik [69] observed a replacement of large centric diatom by smaller diatoms as a consequence of arsenic inputs.

The occasional appearance of abnormalities in the shape of frustules could be interpreted as a damage by the metal and possibly a side effect of defense mechanisms against uptake of the toxicant as shown for ultrastructural alterations by Torres et al. [70] but these diatoms were still able to sustain positive growth,

which has been interpreted by Schmitt-Jansen and Altenburger [71] as a physiological adaptation of these species to the pollution.

Table 7.3 Elemental composition of *Navicula sp.* in control and As treated environment

Element	Composition			
	In Control		As treated	
	wt. (%)	at. (%)	wt (%)	at. (%)
Na	1.43	1.03	6.15	4.68
Mg	0.31	0.21	1.31	0.94
Si	11.86	7.00	20.77	12.93
Cl	0.26	0.12	0.14	0.07
K	0.54	0.23	0.22	0.10
Ca	0.39	0.16	2.18	0.95
Fe	0.20	0.06	0.06	0.02
Zn	0.03	0.01	0.09	0.02
Br	7.27	1.51	1.56	0.34
As	-	-	1.13	0.26

From the above **Table 7.3**, EDX analysis of the diatom frustule treated with As showed the presence of As along with the other elements. So, diatoms can also mineralize Arsenic producing Arsenic nano pores.

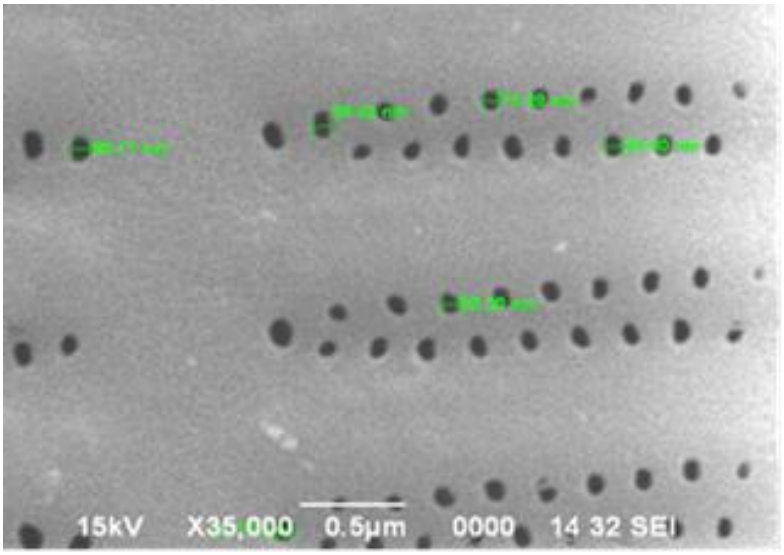

(**A**)

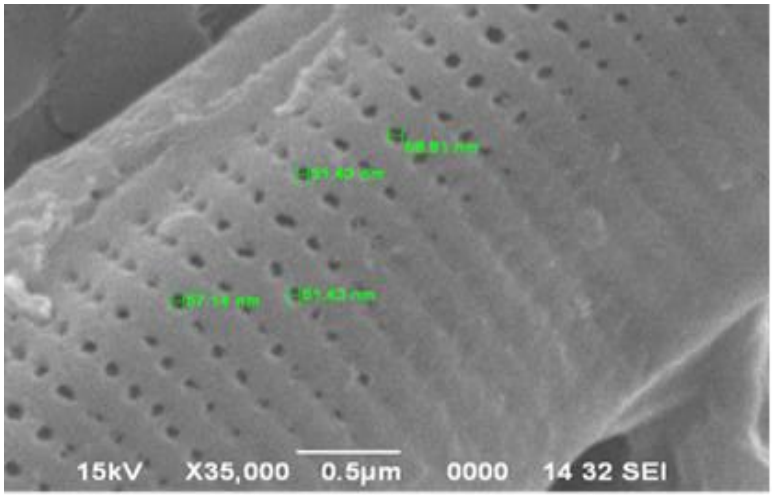

(**B**)

Figure 7.9 SEM images showing the pore sizes of control media (A); (B) Pore sizes of diatom *Navicula* within Arsenic Medium

SEM image analysis shows that the Diatom frustules isolated from the normal media (sodium metasilicate media) (**Figure 7.9A**) has pore size of 80-85 nm whereas frustules isolated from Arsenic media (no sodium metasilicate) (**Figure 7.9B**) has pore size of 45-50 nm. So, the pore size has decreased in case of arsenic medium.

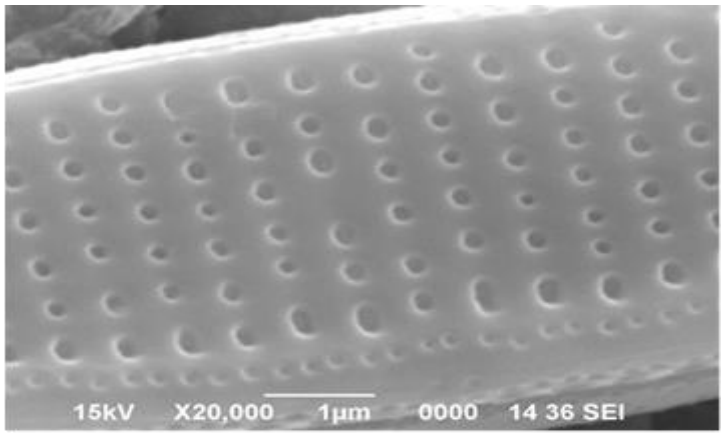

(**A**)

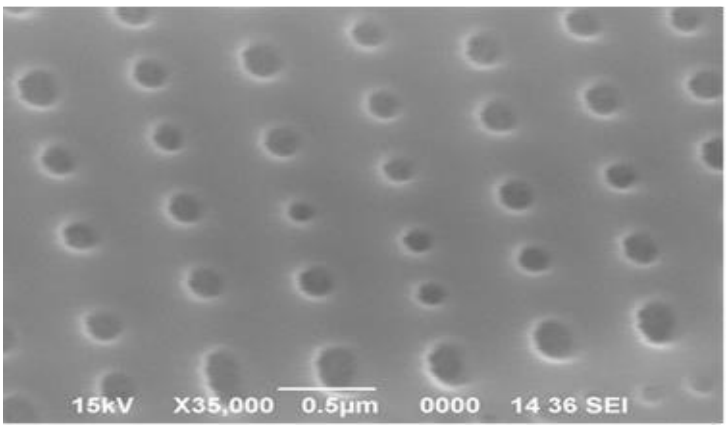

(**B**)

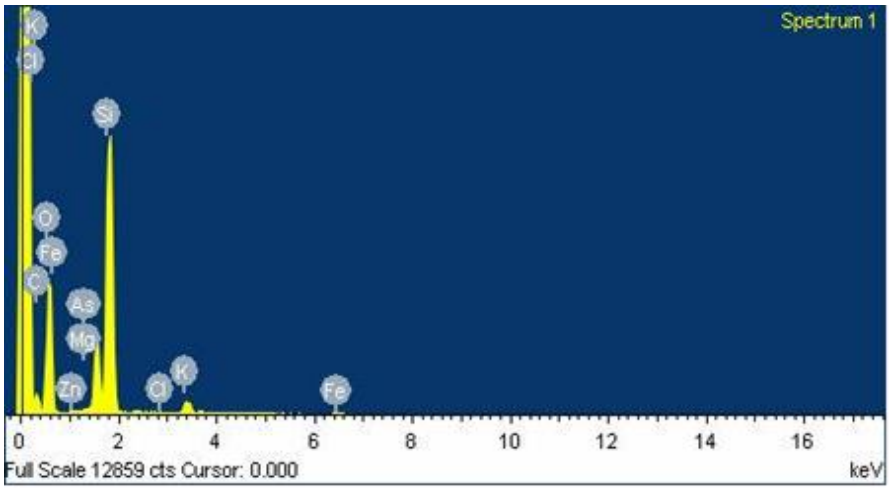

(I)

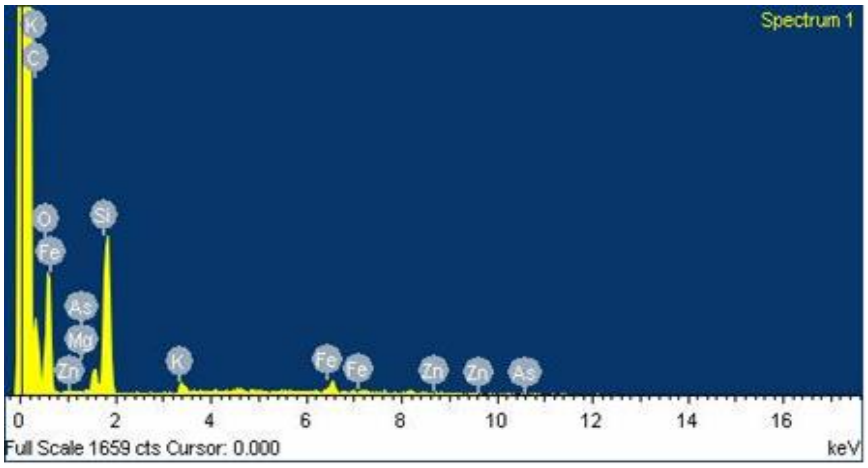

(II)

Figure 7.10 Scanning Electron Microscopic view and EDX of a diatom, *Navicula* sp. It showed nanometer sized in control (A, I) and (B, II) in As media

SEM EDX analysis of the Diatom frustule shows the accumulation of arsenic particles around the pores of the diatom frustule (**Figure 7.10B, II**). On the other hand, the control diatom frustule contain no arsenic (**Figure 7.10A, I**).

7.3.7 XRD Analysis

X-ray powder diffraction (XRD) was used to characterize the crystallographic structure of diatom samples.

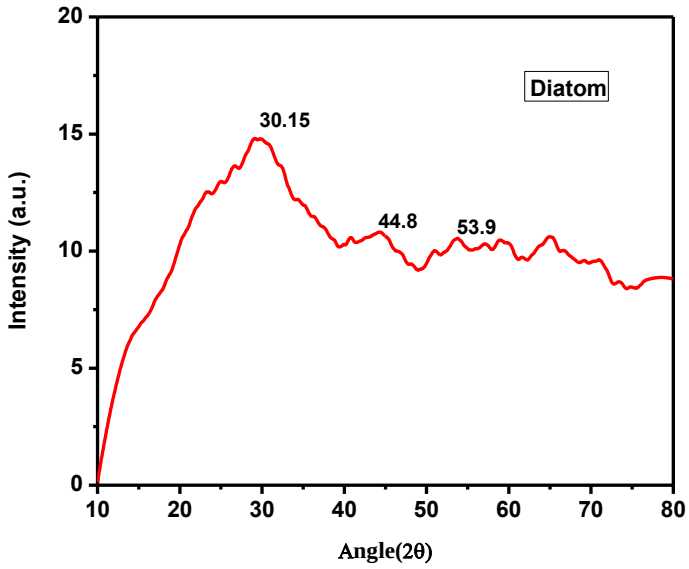

Figure 7.11 XRD pattern of the diatom *Navicula* sp.

The peaks in the XRD profile attributed to the Si substrate. This XRD pattern is due to the amorphous structure of silica. XRD analysis showed that the diatom microparticles mostly consist of amorphous silica. Structural as well as crystallographic information of the diatoms was revealed from X-ray diffraction (XRD) patterns recorded on a Rigaku D/max-2000 diffractometer in the range of diffraction angle (2Θ) between 10^0 to 80^0. The peaks in the Bragg angle of 30.150, 44.8^0 and 53.9^0 corresponds to the presence of silica in the diatom frustules. The experiment was carried out at room temperature. XRD analysis showed that the diatom microparticles mostly consist of amorphous silica with a trace amount of crystalline quartz (**Figure 7.11**).

7.3.8 IR Analysis

The vibrations observed at 468.3 and 1101.1 cm^{-1} correspond to asymmetric stretching modes of Si–O–Si bonds. The vibrations at 2942.9 and 2871.7 cm−1 are associated with the asymmetric and symmetric stretching modes of the –CH2– moiety, respectively, which is directly related to the carbon chain of organosilane

molecules [72, 73]. The –SH stretching vibration occurs at about 2566.8 cm^{-1}. These FTIR results clearly indicate the presence of –SH or $–NH_2$ functional groups on the diatom surface.

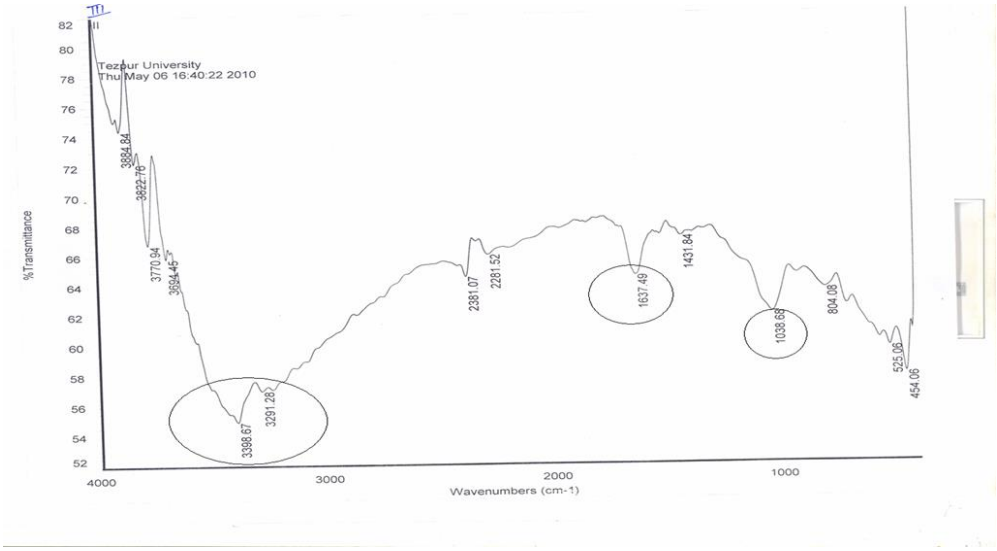

Figure 7.12 FTIR spectra of diatom *Navicula* sp. treated with As solution

FTIR results shows a peak at 1053.70 cm^{-1} which is due to the vibrational stretching of Si-O-Si bond (**Figure 7.12**). Diatom frustules also has OH group which is shown by the peak at 3420 cm^{-1}. Again, presence of carboxyl group gives a vibrational stretching at 1635.96 cm^{-1}.

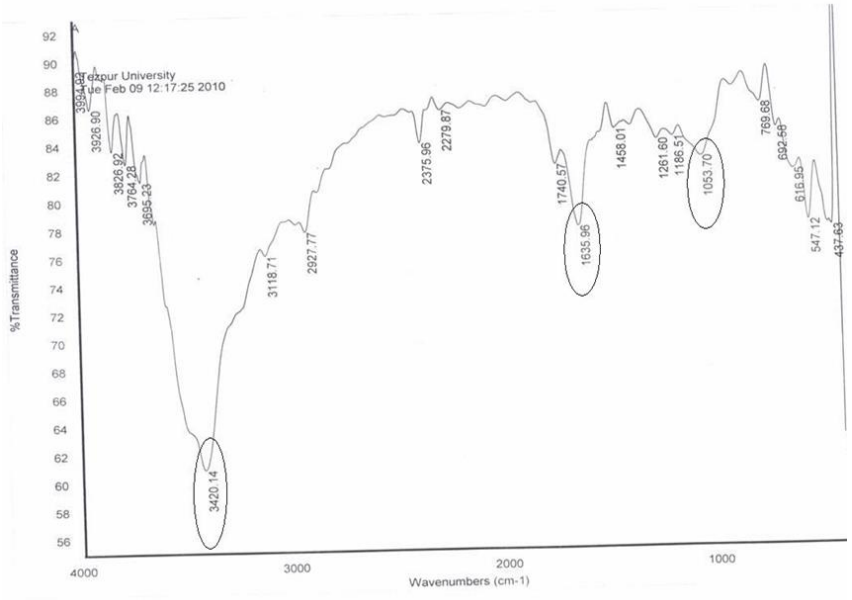

Figure 7.13 FTIR spectra of control diatom group

FTIR analysis shows the Si-O-Si stretching vibration at 1045 cm^{-1} which is lesser than media containing only sodium metasilicate, i.e. normal media (1053 cm^{-1}) (**Figure 7.13**). FTIR results also shows that due to the presence of arsenic, there is a shifting of the peak for carboxyl stretching of fatty acids and amino acids as it gives a peak at 1638.4 cm^{-1} where as in normal media, it is 1635.96 cm^{-1}. FTIR analysis also shows the shifting of vibrational stretching of OH bond at 3457 cm^{-1} where as in normal media, it is 3420 cm^{-1}. FTIR analysis shows that due to the presence of Arsenic, the vibrational stretching of Si-O-Si bond has been shifted and is at 1038 cm^{-1}(**Figure 7.12**) which is lesser than media containing Sodium metasilicate and Arsenic (1045cm^{-1}). Here, Arsenic has affected the vibrational stretching of OH bond more as here the peak is splitted and gives a peak at 3398 cm^{-1} and 3291.28 cm^{-1}. There also has been a shifting in the vibrational stretching of carboxyl group due to which the peak is at 1637.49 cm^{-1} which is different from the normal media (1635.96 cm^{-1}) and media containing Arsenic and sodium metasilicate (1638.4 cm^{-1}).

Table 7.4 Results of diatoms analysis by FT-IR. Band attributions were made according to Bellamy [74] and Colthup et al. [75]

Functional groups	Band (wavelength, cm^{-1}) at 25°C, $\pm$ 5 cm^{-1}	Corresponding structure
Aliphatic	2960	CH_3 asymmetric stretching
	2925	CH_2 asymmetric stretching
	2850	CH_3 symmetric stretching
	1455	C-H bending in CH_2
Proteins	1650	>C=O stretching for primary amids
	1545	N-H bending in amids
Carboxylic acids	~3400	O-H stretching
	1405	C-O stretching in carboxylates
	1735	>C=O stretching of ester or fat acids
Polysaccharides	1086	Ring vibration corresponding to C=O stretching of esters
Hydroxyles	~3400	O-H stretching
Silica	Several bands at 1250–1100, 1070, and at 940, 790	Si-O-Si stretching

7.3.9 Zeta potential measurement

Zeta potential measurement is based on the principle of determining the mobility or electrokinetic velocity of particles as they move through an electric field. It was

used to study the surface charge present on biosorbent particles in aqueous solution.

The zeta potential of control (without As) diatom particles was negative in the pH range from 2 to 11. Despite the acidic nature of –SH groups form a negatively charged conjugate base on the diatom surface [76]. In fact, the influence of heavy metals in the charge alteration of bacteria and yeasts, particularly in the decrease of the negative charges, was reported in many studies. Sadowski [77] described the influence of lead, copper and cadmium in zeta potential modification in the Gram positive *Nocardia* sp. More recently, differences in zeta potential were correlated with the absorption of iron oxide by *Saccharomyces cerevisiae* and *E. coli* [78].

At lower pH, Si–OH deprotonated and contributed to the negative potential upon exposure to aqueous solutions. As a result, the negative zeta potential observed at lower pHs may in part be due to the residual Si–OH on the surface. Zeta potential was reduced from about -15.77 to -12.58 mV.

Figure 7.14 represents the zeta potential profile of As untreated (A) and treated diatom (B). The zeta potential measurement also directly verify the adsorption of As by the diatoms. The controlled diatoms shows a zeta potential value of -15.77 mV. That means that the surface of the diatom is negatively charged. After adsorption of As, the treated diatom shows a zeta potential value of -12.58 mV. It is evident from the decrease in zeta potential that diatoms are good adsorbent for As.

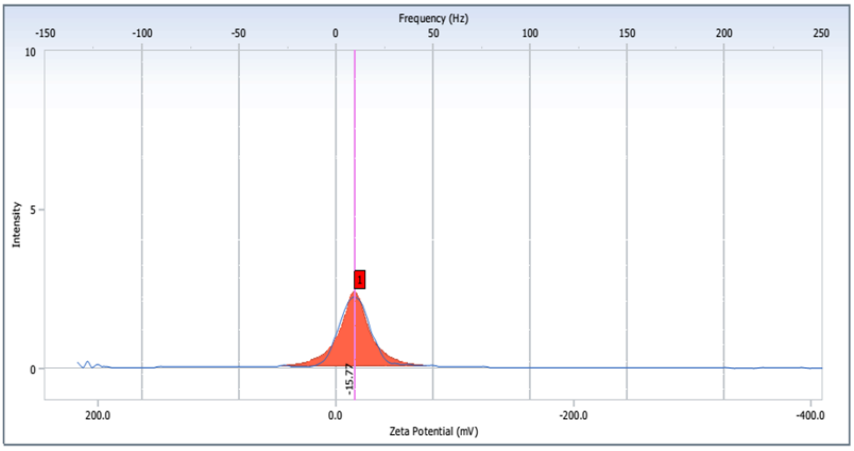

Zeta potential profile of untreated diatom (A).

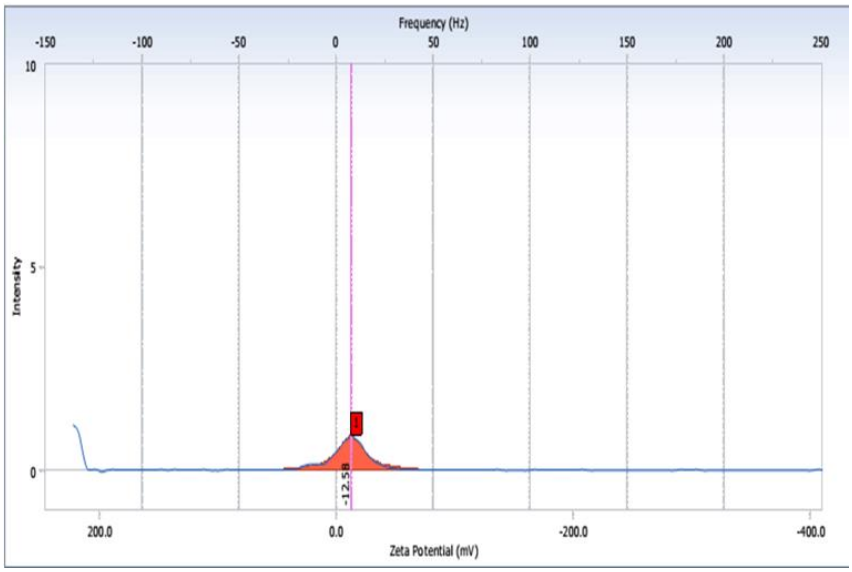

Zeta potential profile of As treated diatom (B).

Figure 7.14 Zeta potential profile of control (A); As treated diatom (B)

The zeta potential was falls sharply below pH^4 (from around -15.77 mV to -12.58 mV at about pH^2). This suggests that surface groups responsible for the high negative zeta-potential begin to interact with protons in solution, lowering the surface charge of the biosorbent particles. Kuyucak [79] reported a similar fall in measured zeta-potential for the brown algae *Sargassum natans*.

Surface adsorption

The characteristics of the cell wall differ among freshwater algae and also between algae species, some of these properties are: cell surface hydrophobicity (hydrophobicity is linked to the polysaccharide content in the cell wall which is correlated to nitrogen and carbon content in the hydrocarbon and inversely correlated to the concentration of oxygen), zeta potential, the presence of anionic or cationic groups (charged carboxyl, phosphate, or amine groups), shape and cell size [80].

The negative surface charge surrounding algal particles in solution, due to the dissociation of acidic functional groups, was also prevalent during zeta-potential measurements carried was carried by zeta analysis. The results indicate the presence of a negative surface charge on algal particles over most of the alkalimetric titration range. The zeta potential of arsenic treated diatom particles falls sharply below pH^4 (from around -60 mV to -10 mV at about pH^2). This suggests that surface groups responsible for the high negative zeta-potential begin to interact with protons in solution, lowering the surface charge of the biosorbent

particles. Kuyucak [81] reported a similar fall in measured zeta-potential for the brown algae *Sargassum natans*.

7.4 Discussion

The algal cell wall may have many functional groups, such as hydroxyl, phosphoryl, amino, carboxyl, sulphydryl etc. which confer negative charge to the cell surface. Most of heavy metal ions in water are in cationic form, thus they get adsorbed on to the cell surface [82, 83]. Since biosorption of heavy metals cations involves binding of metal ions to the anionic groups present on the biomass surface, thus number and ionic state of functional groups present on the biosorption surface play a significant role in heavy metal removal. The nature and presence of functional groups on the biomass surface can be easily ascertained through FTIR analysis. In the FTIR spectrum, one gets peaks at different wave numbers and these peaks results from different characteristics of functional groups.

The band between 1800-1540 cm^{-1} wave numbers is associated with C=O stretching mode in carbonyls, carboxylic acids and lactones, while band between wave numbers 1440-1000 cm^{-1} is assigned to the C-O stretching and O-H bending modes of phenols and carboxylic acids [84, 85].

Gong et al. [86] compared the FTIR spectra of unloaded and lead loaded biomass of *S. maxima* and observed that absorbance peaks of amino and hydroxyl groups stretching vibrations were shifted from 3304 cm^{-1} to about 3285 cm^{-1} in lead loaded biomass. It was suggested that shifting of amino and hydroxyl groups in the spectrum indicated the involvement of these two groups in lead binding.

The cell surface of this alga is a strong electron donator and weak electron acceptor; this combined with the hydrophobicity of the cell can be linked to its low concentration of polysaccharides. The iso-electric point in the cell wall is 2.9 (measured as the zeta potential). This indicates that at neutral pH the cell surface is negatively charged therefore attracting positively charged molecules such as metal ions which was found in our study (**Figure 7.14**).

7.5 Conclusion

It is very difficult to assess the effects of As on diatom biofilms in laboratory experiments. Therefore, this study was carried out to obtain an approximation of the toxicity of As at different stages in the development of the community using experimental microcosms. It is difficult to account for the differences between treatments because the physicochemical variables exhibited similar trends for all

treatments, with the exception of growth, which increased more in one system. Despite this, it was observed that: (i) diatom biofilms have a good accumulation capacity, and their growth seems to be lowered by As exposure, (ii) shifts in species composition and decreases in species richness may be attributed to As exposure, and (iii) changes in diatom morphology (deformities) are much more frequently observed in high As-treated microcosms (55mg/L).

An important finding in this respect from the current study is the aggravating influence of algae on the impacts of arsenic exposure in diatom. Bioremediation of arsenic contaminated waters using aquatic algae should therefore be carried out with consideration of entire ecosystem effects. Such multidisciplinary, cross-taxon research is crucial for understanding the impacts of arsenic toxicity and thus restoration of aquatic ecosystems.

References

1. Werner, D. *The Biology of Diatoms*, Botanical Monographs. Univ. of California Press, (ed), 1977, Vol. 13, 498.
2. Round, F. E., Crawford, R. M. & Mann, D. G. *The Diatoms: Biology and Morphology of the Genera*, Cambridge University Press, 1990.
3. Prescott, G.W. *Algae of the Western Great Lakes Area*, Michigan State University, USA, 1975, 998-1012.
4. Rai, S.K. Taxonomic Studies on Some Freshwater Diatoms from the Eastern Terai Region, Nepal, *Our Nature* **4**, 10--19, 2006.
5. Dixit, S. S., et al. Diatoms: powerful indicators of environmental change, *Environ. Sci. Technol.* **26**(1), 22--33, 1992.
6. Gordon, R., & Drum, R.W. The chemical basis for diatom morphogenesis, *Int. Rev. Cytol.* **150**, 243--372, 1994.
7. Gordon, R. & Drum, R.W. Stability of colloidal silica: I. Effect of simple electrolytes, *Int. Rev. Cytol*. **150**, 243--372, 1994.
8. Preisig, H. R. Siliceous structures and silicification in flagellated protists, *Protoplasma* **181**, 29--42, 1994.
9. Conley, D.J., & Kilham, S.S. Differences in silica content between marine and freshwater diatoms, *Limnol. Oceanogr*. **34**(1), 205--213, 1989.
10. Pickett-Heaps, J., Schmid, A.-M.M., & Edgar, L.A. In FE Round, DJ Chapman, eds, *The Cell Biology of Diatom Valve Formation*, Vol 7. Biopress Ltd., Bristol, UK, 1990, 1–168.

11. Vrieling, E. G., et al. Diatom silicon biomineralization as an inspirational source of new approaches to silica production, *J. Biotechnol*. **70**, 39--51, 1999.
12. Davis, A., et al. An analysis of soil arsenic records of decision, *Environ. Sci. Technol*. **35**, 2401--2406, 2001.
13. Ferguson, J. F. & Gavis, J. `A review of the arsenic cycle in natural waters, *Water res.* **6**(11), 1259-1274, 1972.
14. Hellweger, F.L., & Lall, U. Modelling the effect of algal dynamics on arsenic speciation in Lake Biwa, *Environ. Sci. Technol.* **38**, 6716--6723, 2004.
15. Rahman, M. A., & Hasegawa, H. Arsenic in freshwater systems: influence of eutrophication on occurrence, distribution, speciation, and bioaccumulation, *Appl. Geochem*. **27**, 304--314, 2012.
16. Rahman, M. A., et al. Bioaccumulation, bio transformation and trophic transfer of arsenic in the aquatic food chain, *Environ. Res*. **116**,118--135, 2012.
17. Yin, X., et al. Characterization of arsenate transformation and identification of arsenate reductase in a green alga *Chlamydomonas reinhardtii*, *J. Environ. Sci*. *China* **23**, 1186--1193, 2011.
18. Yin, X. X., et al. Accumulation and transformation of arsenic in the blue-green alga *Synechocysis* sp PCC6803, *Water Air Soil Pollut*. **223**, 1183--1190, 2012.
19. Levy, J. L., et al. Toxicity, biotransformation, and mode of action of arsenic in two freshwater microalgae (*Chlorella* sp. and *Monoraphidium arcuatum*), *Environ. Technol. Chem*. **24**, 2630--2639, 2005.
20. Favas, P. J.C., Pratas, J., & Prasad, M.N.V. Accumulation of arsenic by aquatic plants in large-scale field conditions: opportunities for phytoremediation and bioindication, *Sci. Total Environ*. **433**, 390--397, 2012.
21. Wang, N.-X., et al. Toxicity and bioaccumulation kinetics of arsenate in two freshwater green algae under different phosphate regimes, *Water Res*. **47**, 2497--2506, 2013.
22. Rosen, B.P. Biochemistry of arsenic detoxification, *FEBS Lett*. **529**, 86--92, 2002.
23. Morin, S., et al. Dynamics of benthic diatom colonization in a cadmium/zinc-polluted river (Riou-Mort France), *Fundam. Appl. Limnol*. **168**, 179--187, 2007.
24. Jurewicz, S, & Buikema, A.L. Effects of arsenate on algae, *Daphnia* and mosquito fish, *Va. J. Sci*. **31**, 124, 1980.

25. Vocke, R.W., et al. Growth responses of selected freshwater algae to trace elements and scrubber ash slurry generated by coal-fired power plants, *Water Res.* **14**, 141--150, 1980.
26. Fargošová, A. Comparative toxicity of five metals on various biological subjects, *Bull. Environ. Contam. Toxicol.* **53**, 317--324, 1994.
27. Morin, S., et al. Consistency in diatom response to metal-contaminated environments, In: Guasch, H., Ginebreda, A., Geiszinger, A. (Eds.), *Emerging and Priority Pollutants in Rivers*, The Handbook of Environmental Chemistry, vol. 19. Springer, Heidelberg, 2012.
28. Cattaneo, A., et al. Organisms' response in a chronically polluted lake supports hypothesized link between stress and size, *Limnol. Oceanogr*. **43**(8), 1938--1943, 1998.
29. Cattaneo, A., et al. Diatom taxonomic and morphological changes as indicators of metal pollution and recovery in Lac Dufault (Québec, Canada), *J. Paleolimnol*. **32**, 163--175, 2004.
30. Pedersen, M., G. M. Roomans, M. Andren, Ä. Lignell, G. Lindahl, K. Wallström, Ä. Forsberg. *X-ray microanalysis of metals in algae — a contribution to the study of environmental pollution*. Scanning Electron Microscopy/I98f/If: 499-509, 1981.
31. Lee, R.D. X-ray microanalysis. In *Scanning Electron Microscopy and X-ray Microanalysis*, Prentice-Hall, Inc.: New Jersey, 1993, 329–409.
32. Goldstein, J.I. Scanning electron microscopy and X-ray microanalysis, a text of biologist, materials scientists, and geologists, 1982.
33. Newman, M. C., et al. Geochemical factors complicating the use of aufwuchs to monitor bioaccumulation of arsenic, cadmium, chromium, copper and zinc, *Water Res*.**19**, 1157--1165, 1985
34. Schorer, M., & Eisele, M. Accumulation of inorganic and organic pollutants by biofilms in the aquatic environment, *Wat. Air. Soil. Pollut*. **99**, 651--659, 1997.
35. Chien, J.T. Some aspects of water quality in a polluted lowland river in relation to the intracellular chemical level in planktonic and epilithic diatom, *Water Res.* **38**, 1779--1790, 2004.

36. Boyle, E. A., et al. Trace metals and radium in the Gulf of Mexico: an evaluation of river and continental shelf sources, *Earth Planet. Sci. Lett.***69**, 69--87, 1984.
37. Campbell, P.G.C. Interactions between trace metals and aquatic organisms: a critique of the free-ion activity model. Metal speciation and bioavailability in aquatic systems, John Wiley & Sons, Chichester, 1995, 45–102.
38. Aksu, Z., & Wong, Y.S. Biosorption of heavy metals by microalgae in batch and continuous systems. In: Algae for waste water treatment. Springer Germany 99, 37, 1998.
39. Pavasant, P., et al. Biosorption of Cu^{2+}, Cd^{2+}, Pb^{2+}, and Zn^{2+} using dried marine green macroalga *Caulerpa lentillifera*, *Bioresour. Technol*. **97**(18): 2321--2329, 2006.
40. Gupta, V.K., et al. Biosorption of chromium (VI) from aqueous solutions by green algae Spirogyra species, *Water Res*. **35**, 4079--4085, 2001.
41. Gupta, V.K., & Rastogi, A. Biosorption of lead (II) from aqueous solutions by non-living algal biomass *Oedogonium* sp. and *Nostoc* sp.--a comparative study, *Colloid*. *Surface B* **64**(2), 170-178, 2008.
42. Maher, W. et al. Arsenic concentrations and speciation in the tissues and blood of sea mullet (*Mugil cephalus*) from Lake Macquarie NSW, Australia, *Marine Chemistry* **68**, 169--182, 1999.
43. Ray, R., & Little, B. Environmental electron microscopy applied to biofilms. In: Lens P, Moran AP, Mahony T, Stoodley P & O'Flaherty V (Eds) *Biofilms in Medicine, Industry and Environmental Biotechnology: Characteristics, Analysis and Control*, IWA publishing, London, UK, 2003, 331–351.
44. White, C., & Gadd, G.M. Copper accumulation by sulfate reducing bacterial biofilms, *FEMS Microbiol*. *Lett.* **183**, 313--318, 2000.
45. Yamaguchi, T., et al. Microbial ecological significance of sulfide precipitation within anaerobic granular sludge revealed by micro-electrodes study, *Water Res.* **35**, 3411--3417, 2001.
46. Karthikeyan, S., & Beveridge, T.J. *Pseudomonas aeruginosa* biofilms react with and precipitate toxic soluble gold, *Environ. Microbiol.* **4**, 667--675, 2002.
47. Lai, S.D., Chen, P.C., & Hsu, H.K. Benthic algae as monitors of heavy metals in various polluted rivers by energy dispersive X-ray spectrometer, *J. Environ. Sci. Health A* **38**, 855--866, 2003.

48. Chien, J.T. Some aspects of water quality in a polluted lowland river in relation to the intracellular chemical level in planktonic and epilithic diatom, *Water Res.* **38**, 1779--1790, 2004.
49. Nakanishi, Y., et al. Heavy-metal pollution and its state in algae in Kakehashi River and Godani River at the foot of Ogoya mine, Ishikawa, *Anal. Sci*. **20**, 73--78, 2004.
50. Mehta, S.K., & Gaur, J.P. Use of Algae for Removing Heavy Metal Ions from Wastewater: Progress and Prospects, *Critical Reviews in Biotechnology* **25**, 113--152, 2005.
51. Aksu, Z., & Tezer, S. Biosorption of reactive dyes on the green alga *Chlorella vulgaris*, *Process Biochemistry* **40**, 1347--1361, 2005.
52. Gélabert, A., et al. Study of diatoms/ aqueous interface. I. Acid-base equilibria and spectroscopic observation of freshwater and marine species, *Geochimica et Cosmochimica Acta* **68**, 4039--4058, 2004.
53. Gélabert, A., et al. Interaction between zinc and freshwater and marine diatom species: Surface complexation and Zn isotope fractionation, *Geochimica et Cosmochimica Acta* **70**, 839--857, 2006.
54. Pokrovsky, O. S., et al. Speciation of Zn associated with diatoms using X-ray absorption spectroscopy, *Environ. Sci. Technol*. **39**, 4490--4498, 2005.
55. Guillard, R.R.L., & Lorenzen, C.J. Yellow-green algae with chlorophyllide c. *J. Phycol*. **8**, 10--14, 1972.
56. Gogoi, A., et al. Laboratory measurements of light scattering by tropical fresh water diatoms, *Quantitative Spectroscopy and Radiative Transfer* **110**, 1566--1578, 2009.
57. Behra, R., et al. Copper and Zinc content of periphyton from two rivers as a function of dissolved metal concentration, *Aquatic Sciences* **64**, 300--306, 2002.
58. Meylan, S., et al. Influence of metal speciation in natural freshwater on bioaccumulation of copper and zinc in periphyton: a microcosm study, *Environ. Sci. Technol*. **38**, 3104--3111, 2004.
59. Toumi, A., et al. Heavy metal removal in waste stabilization ponds and high rate ponds, *Water.Sci.Technol*. **42**, 17--21, 2000.

60. Jeffrey, S.W., & Humphrey, G.F. New spectrophotometric equations for determining chlorophylls a, b, c_1 and c_2 in higher plants, algae and natural phytoplankton, *Bioch. Physiol. Pflanz*. **167**, 191--194, 1975.
61. Doshi, H., et al. Bioaccumulation of heavy metals by green algae, *Curr. Microbiol*. **56**, 246--255, 2008.
62. Ivorra, N., et al. Responses of biofilms to combined nutrient and metal exposure, *Environ. Toxicol. Chem*. **21**, 626--632, 2002.
63. Soeprobowati, T.R., & Hariyati, R. Bioaccumulation of Pb, Cd, Cu, and Cr by *Porphyridium cruentum* (S.F. Gray) Nägeli, *Int. J. Mar. Sci. Eng*. **3**(27), 212--218, 2013.
64. Banvalvi, G. Cellular effects of heavy metals, Springer, London, 201, 364,
65. Roosens, N., et al. Natural variation in cadmium tolerance and its relationship to metal hyperaccumulation for seven populations of *Thlaspi caerulescens* from Western Europe, *Plant Cell Env*. **26**, 1657--1672, 2003.
66. Mayama, S., & Kuriyama, A. Diversity of mineral cell coverings and their formation processes: a review focused on the siliceous cell coverings, *J. Plant Res.* **115**, 289--295, 2002.
67. Schmid, A. M. Aspects of morphogenesis and function of diatom 1 cell walls with implications for taxonomy, *Protoplasma* **181**, 43--60, 1994.
68. Pe´rez-Rama, M., et al. Class III metallothioneins in response to cadmium toxicity in the marine microalga *Tetraselmis suecica* (Kylin) Butch, *Environ. Toxicol. Chem*. **20**, 2061--2066, 2006.
69. Sanders, J., & Cibik, S. Response of Chesapeake Bay phytoplankton communities to low levels of toxic substances, *Mar. Pollut. Bull*. **19**(9), 439--444, 1988.
70. Torres, E., et al. Effect of cadmium on growth, ATP content, carbon fixation and ultrastructure in the marine diatom *Phaeodactylum tricornutum* Bohlin, *Water Air Soil Pollut.* **117**, 1-14, 2000.
71. Schmitt-Jansen, M., & Altenburger, R. Toxic effects of isoproturon on periphyton communities - a microcosm study, Estuar, *Coast. Shelf Sci.* **62**, 539--545, 2005.
72. Liang, X., et al. Preparation, characterization of thiol-functionalized silica and application for sorption of $Pb^{2+}$and Cd^{2+}, *Colloids Surf. A*. **349**, 61--68, 2009.

73. Finocchio, E., et al. Adsorption of trimethoxysilane and of 3-mercaptopropyltrimethoxysilane on silica and on silicon wafers from vapor phase: an IR study, *Langmuir* **23**, 2505--2509, 2007.
74. Bellamy, L. J. *The Infrared Spectra of Complex Molecules*, Chapman and Hall, 1975.
75. Colthup N. B., et al. *Introduction to Infrared and Raman Spectroscopy*, Academic Press, 1975.
76. Kuo, C, H., et al. Effect of surface chemical composition on the surface potential and iso-electric point of silicon substrates modified with self-assembled monolayers, *Phys. Chem. Chem. Phys*. **13**, 3649--3653, 2011.
77. Sadowski, Z. Effect of biosorption of Pb (II), Cu (II) and Cd (II) on the zeta potential and flocculation of *Nocardia* sp, *Miner. Eng.* **14**, 547--552, 2001.
78. Schwegmann, H., et al. Influence of the zeta potential on the sorption and toxicity of iron oxide nanoparticles on *S. cerevisiae* and *E. coli*, *J. Colloid Interface Sci*. **347**, 43--48, 2010.
79. Kuyucak, N. Algal Biosorbents for Gold and Cobalt, PhD thesis, McGill University, 1987.
80. Hadjoudja, S., Deluchat, V., & Baudu, M. Cell surface characterisation of *Mycrocystis aeruginosa* and *Chlorella vulgaris*, *J. Colloid Interface Sci.* **342**, 293--299, 2010.
81. Kuyucak, N. and Volesky, B. Desorption of cobalt-laden algal biosorbent. *Biotechnology and Bioengineering*, **33**, 815--822, 1989.
82. Skowronski, P., & Ska, B. Relationship between acid-soluble thiol peptides and accumulated Pb in the green alga *Stichococcus bacillaris*, *Aquat. Toxicol*. **50**, 221–230, 2000.
83. Mehta, S.K., & Gaur, J.P. Use of algae for removing heavy metal ions from wastewater: Progress and prospects, *Crit. Rev. Biotechnol*. **25**, 113--152, 2005.
84. Gardea-Torresdey, J.L., et al. Infrared and X-ray adsorption spectroscopic studies on the mechanism of chromium (III) binding to alfalfa biomass, *Microchem. J*. **71**, 157--166, 2002.
85. Mohan, D., & Pittman Jr, C.U. Activated carbons and low cost adsorbent for remediation of tri and hexavalent chromium from water, *J. Hazard. Mater*. **137**, 762--811, 2006.
86. Gong, R., et al. Lead biosorption and desorption by intact and pretreated *Spirulina maxima* biomass, *Chemosphere* **58**, 125--130, 2005.